



Published in final edited form as:

*J Pineal Res.* 2016 August ; 61(1): 69–81. doi:10.1111/jpi.12328.

## GABAergic signaling in the rat pineal gland

Haijie Yu<sup>1,\*</sup>, Sergio G. Benitez<sup>2,\*</sup>, Seung-Ryoung Jung<sup>1</sup>, Luz E. Farias Altamirano<sup>2</sup>, Martin Kruse<sup>1</sup>, Jong-Bae Seo<sup>1</sup>, Duk-Su Koh<sup>1</sup>, Estela M. Muñoz<sup>2,‡</sup>, and Bertil Hille<sup>1,‡</sup>

<sup>1</sup>Department of Physiology and Biophysics, University of Washington School of Medicine, Seattle, WA, USA

<sup>2</sup>Laboratory of Neurobiology: Chronobiology Section, Institute of Histology and Embryology of Mendoza (IHEM-CONICET), School of Medicine, National University of Cuyo, Mendoza, Argentina

### Abstract

Pinealocytes secrete melatonin at night in response to norepinephrine released from sympathetic nerve terminals in the pineal gland. The gland also contains many other neurotransmitters whose cellular disposition, activity, and relevance to pineal function are not understood. Here we clarify sources and demonstrate cellular actions of the neurotransmitter  $\gamma$ -aminobutyric acid (GABA) using Western blotting and immunohistochemistry of the gland and electrical recording from pinealocytes. GABAergic cells and nerve fibers, defined as containing GABA and the synthetic enzyme GAD67, were identified. The cells represent a subset of interstitial cells while the nerve fibers were distinct from the sympathetic innervation. The GABA<sub>A</sub> receptor subunit  $\alpha 1$  was visualized in close proximity of both GABAergic and sympathetic nerve fibers as well as fine extensions among pinealocytes and blood vessels. The GABA<sub>B1</sub> receptor subunit was localized in the interstitial compartment but not in pinealocytes. Electrophysiology of isolated pinealocytes revealed that GABA and muscimol elicit strong inward chloride currents sensitive to bicuculline and picrotoxin, clear evidence for functional GABA<sub>A</sub> receptors on the surface membrane. Applications of elevated potassium solution or the neurotransmitter acetylcholine depolarized the pinealocyte membrane potential enough to open voltage-gated Ca<sup>2+</sup> channels leading to intracellular calcium elevations. GABA repolarized the membrane and shut off such calcium rises. In 48–72-h cultured intact glands, GABA application neither triggered melatonin secretion by itself nor affected norepinephrine-induced secretion. Thus strong elements of GABA signaling are present in pineal glands that make large electrical responses in pinealocytes, but physiological roles need to be found.

---

**For correspondence:** Bertil Hille, Department of Physiology and Biophysics Box 357290, University of Washington School of Medicine, Seattle, WA 98195-7290, USA. PHONE: 206-543-8639, FAX: 206-685-0619, hille@uw.edu.

\*co first authors

‡co last authors

### Author contributions

B.H., E.M. and D.S.K. designed the experiments; H.Y., S.G.B., S.R.J., L.E.F.A., M.K., and J.B.S. collected the data; B.H. and E.M. wrote the paper.

## Keywords

pineal gland; GABA; GABA<sub>A</sub> receptor; GAD67; bicuculline; melatonin secretion; membrane potential

---

## Introduction

This study explores signaling by the neurotransmitter  $\gamma$ -aminobutyric acid (GABA) in the rat pineal gland. The pineal gland secretes the hormone melatonin from pinealocytes throughout the night. The secretion has a circadian rhythm primarily because it is driven by the nocturnal release of norepinephrine (NE) from pinealopetal sympathetic nerve fibers of the superior cervical ganglia [1–3]. NE acting through  $\alpha_1$ - and  $\beta_1$ -adrenergic receptors induces expression of the rate-limiting enzyme of melatonin synthesis, arylalkylamine N-acetyltransferase (AANAT) [4, 5]. AANAT converts serotonin (5-HT) into N-acetylserotonin (NAS), and a second enzyme hydroxyindole O-methyltransferase generates melatonin. Since both melatonin and N-acetylserotonin are highly membrane permeant [6], their synthesis is synonymous with secretion. The pineal gland contains several cell types [7, 8] that we now enumerate because we study them here by immunohistochemistry. Principal among them are the secretory pinealocytes, evolutionarily derived from photoreceptors (see references in Klein, 2004[9]). Pinealocytes are ovoid cells (7–12  $\mu\text{m}$  diameter) with a highly lobulated euchromatic nucleus, one or more evident nucleoli, and an abundant cytoplasm, with granules, small clear vesicles, and synaptic ribbons (like photoreceptors); three to five processes having club-like endings are observed [7, 8, 10, 11] but pinealocytes fail to form or receive classical synapses. Much less abundant are smaller interstitial cells of various kinds that often have macroglia-like or microglia-like properties with round or triangular more compact nuclei and narrow and long processes. Finally there are nerve fibers that form bundles, mostly unmyelinated, in perivascular spaces. A major subset of nerve endings are tyrosine hydroxylase positive; they disappear after bilateral superior cervical sympathectomy and contain granules and vesicles that are sensitive to reserpine. These are the NE-secreting sympathetic fibers. Except for the prominent action of NE on pinealocytes, very little is known about the interactions among pineal cells and the roles of a vast number of other neurotransmitters whose actions need further characterization. For example Simonneaux and Ribelayga [2] describe more than 15 neuropeptides detected in the pineal gland (see also Møller and Baeres, 2002[8]), a few of which alter melatonin secretion when applied exogenously. In addition there is some information on the presence and/or actions of the classical neurotransmitters: glutamate, acetylcholine, GABA, and other monoamines. Do these molecules refine the circadian and seasonal secretion of melatonin [4, 5], or the changes of thyroid hormone action by modulating the rhythm of type II iodothyronine deiodinase [12, 13], or other less characterized pineal functions?

Here we consider GABA in mammalian pineal glands. In the adult nervous system, GABA is generally an inhibitory neurotransmitter acting on two broad classes of receptors. The ionotropic GABA<sub>A</sub> receptors are pentameric, Cl<sup>-</sup>-permeable anion channels with subunits coded by 19 genes [14]; GABA-induced ion channel opening is antagonized by bicuculline (except for the three rho subunits), blocked by picrotoxin, and potentiated by

benzodiazepines. By contrast, the metabotropic GABA<sub>B</sub> receptors are obligate heterodimeric G-protein coupled receptors [15]; they are activated by baclofen and antagonized by CGP 55845. Although to this day we lack a conclusive understanding of the significance of GABA in the pineal gland, older work in different species including rat, gerbil, and bovine already presented significant and sometimes contradictory evidence for its uptake, localization, synthesis, release, and possible action in the gland [16–24]. For uptake and release, this work reported: avid <sup>3</sup>H-GABA uptake in the gland into gliocytes, but not into sympathetic axons or pinealocytes [16, 17] or alternatively into a small fraction of pinealocytes [22]; plasma membrane GABA transporters GAT1 and GAT3 in pinealocytes and some interstitial glial cells [23]; vesicular inhibitory amino acid transporter VIAAT in subpopulations of astrocytes and microglia but not in pinealocytes [24]; and release of <sup>3</sup>H-GABA from the gland by KCl depolarization and by activation of  $\alpha$ -adrenergic receptors [21, 22]. For synthesis, the literature reports the presence of glutamic acid decarboxylase (GAD), the enzyme of GABA synthesis in rat pineal cells and not in nerve fibers, because it persists in glands collected after chronic pineal stalk section or removal of the superior cervical ganglia or after 48-h in culture [17], and in gerbil it is said to co-localize with a pinealocyte marker [23]. Alternatively, Sakai et al. [25] reported that GABA is present in central nerve fibers that innervate the pineal gland through the stalk but not in the superior cervical ganglion-derived sympathetic fibers or in pineal cell bodies in various species; in rat pineal gland, GABA-positive endings making synaptic contacts with pinealocytes were not observed. For physiological actions, the literature reports the presence of benzodiazepine binding sites (GABA<sub>A</sub> receptors) and GABA-induced and picrotoxin-blocked <sup>36</sup>Cl<sup>-</sup> uptake [22]. For GABA actions on measures of melatonin synthesis in rat pineal glands, previous studies are inconsistent [22]. Mata et al. [17] looked for GABA actions on control of the AANAT enzyme both in freshly isolated and in 48-hour cultured rat pineal glands. With a variety of experiments they concluded that GABA “does not influence or modulate the adrenergic regulation of pineal [AANAT] activity” either by pre or postsynaptic actions. On the other hand Balemans et al. [20] proposed a dual effect of GABA on melatonin synthesis. They measured <sup>3</sup>H-acetyl incorporation from bath applied acetyl-CoA into melatonin secreted from freshly isolated night (ZT19) pineal glands (without additional NE stimulation). If GABA (10  $\mu$ M) and the <sup>3</sup>H-acetyl donor were applied simultaneously for 60 min, GABA enhanced <sup>3</sup>H incorporation by 25%, whereas if GABA was applied for 20 min initially followed by both agents for 40 min, GABA depressed <sup>3</sup>H incorporation by 30%. Finally, Rosenstein et al. [21] measured secretion of melatonin from freshly isolated day (ZT3-6) pineal glands cultured initially for 3 h with GABA (10  $\mu$ M) alone before being stimulated by NE (10  $\mu$ M) plus GABA for 3 h. GABA reduced the melatonin secretion by 57% [21, 22]. Recent global transcriptome analyses of entire pineal glands identified mRNA for several relevant genes (some of them exhibiting daily variations): the GABA<sub>A</sub> channel, in order of abundance:  $\alpha_1$ -,  $\rho_1$ -,  $\beta_3$ -,  $\gamma_2$ -, and  $\rho_2$ -subunits (*Gabra1*, *Gabbr1*, *Gabrb3*, *Gabrg2*, and *Gabbr2*; [3, 26, 27]), the GABA<sub>B</sub> receptor subunits 1 and 2 (*Gabbr1* and *Gabbr2*; [3]), and, with low average abundance, the GAD67 and GAD65 enzyme genes *Gad1* and *Gad2* [3, 28], among other GABAergic markers.

Our work seeks to complete some missing parts of this description. We determine which cells and structures in the pineal gland contain the elements of GABAergic transmission, we

make the first electrophysiological demonstration of ionotropic GABA<sub>A</sub> receptors in pinealocytes, and we reveal powerful effects on the membrane potential and intracellular Ca<sup>2+</sup> dynamics.

## Materials and Methods

### Animals and cell culture

For immunohistochemistry and Western blot experiments done in Mendoza, male Wistar rats (12 – 16 weeks old) were housed under a 12:12 light-dark cycle (light on at 7:00 AM, *Zeitgeber* Time, ZT0) and water and food *ad libitum*. Animals were sacrificed by decapitation after ketamine/xylazine (50 and 5 mg per kg of body weight, respectively) anesthesia according to protocols approved by the Institutional Animal Care and Use Committee, School of Medicine, National University of Cuyo, Mendoza, Argentina. The pineal gland was collected at ZT6 (midday) and under dim red light at ZT18 (midnight), and immediately fixed in 4% paraformaldehyde in phosphate-buffered saline at 4°C for immunohistochemistry or immediately frozen at –80°C for Western blot. The cerebellum was collected as a positive control at the same time.

For electrophysiological experiments and melatonin secretion measurements done in Seattle, male Sprague-Dawley rats (6 – 12 weeks old) were maintained in standard laboratory conditions under a 14:10 light-dark cycle (light on at 6:00 AM, ZT0). Animals were sacrificed between 8:30 and 10:00 AM (ZT2.5-4). Briefly, pineal glands were removed from rats killed by CO<sub>2</sub> according to guidelines approved by the University of Washington Institutional Animal Care and Use Committee (IACUC). For gland culture, the intact glands were kept at 37°C in a 5% CO<sub>2</sub> incubator in M199 medium (Life Technologies, Carlsbad, CA, USA). For dissociated pinealocytes, cells were dispersed as described previously [29, 30]. Briefly, the glands were dissected into small pieces and treated with 4 mg/ml collagenase (Type I, Sigma-Aldrich, St. Louis, MO, USA) in Hank's buffered saline solution (HBSS, Life Technologies) containing 20 mM HEPES and 1 mg/ml bovine serum albumin (BSA, Sigma-Aldrich) for 30–40 min at 37°C. The digested tissue was dispersed by trituration in a Ca<sup>2+</sup>-free HBSS solution containing 1 mM EGTA, 20 mM HEPES, and 10 mg/ml BSA. Within 2 h of removal of the gland, the isolated cells were plated on glass coverslips and kept at 37°C in the incubator with RPMI 1640 culture medium (Life Technologies) containing 10 mM glucose, 10% fetal bovine serum (FBS), 100 µg/ml streptomycin, and 100 IU/ml penicillin (Life Technologies). Electrophysiological recording with fast solution changes usually requires tightly adherent cells, so for isolated pinealocytes it was necessary to wait for at least 24 hours after cell dispersion. Recordings made 24, 48, or 72 hours after pinealocyte isolation were indistinguishable.

### Solutions and drugs

For voltage-clamp electrophysiology, the standard external solution contained (in mM): 160 NaCl, 2.5 KCl, 2 CaCl<sub>2</sub>, 1 MgCl<sub>2</sub>, 10 HEPES and 8 D-glucose, pH 7.4 adjusted with NaOH. The internal pipette solution contained (in mM): 140 CsCl, 1 MgCl<sub>2</sub>, 1.1 CaCl<sub>2</sub>, 3 EGTA, 10 HEPES, 3 MgATP, 0.3 NaGTP, pH 7.2 adjusted with CsOH. For one experiment with reduced Cl<sup>-</sup> in the external solution, 148.5 mM of the NaCl was replaced with equimolar

Na-gluconate leaving only 20 mM  $\text{Cl}^-$ , and the internal solution contained (in mM): 130 Cs-glutamate, 10 CsCl, 1  $\text{MgCl}_2$ , 3.7  $\text{CaCl}_2$ , 10 EGTA, 10 HEPES, 3 MgATP, 0.3 NaGTP, pH 7.2 adjusted with CsOH. In the current-clamp experiments, done with the perforated patch configuration, the pipette solution had reduced  $\text{Cl}^-$  and contained: 130 K-glutamate, 10 KCl, 10 HEPES, 1  $\text{MgCl}_2$ , 0.1 EGTA, 3 MgATP, 0.3 NaGTP, pH 7.2 adjusted with KOH. For all experiments, extracellular solutions were exchanged by a fast local perfusion system that allowed complete exchange within 0.5 s [31]. GABA and bicuculline methiodide were purchased from Sigma-Aldrich; CGP 55845, muscimol, picrotoxin, from Tocris Bioscience (Minneapolis, MN, USA), and fura-2 AM salt from Life Technologies.

## Immunohistochemistry

Samples were processed for immunohistochemistry as described [32, 33]. Briefly, fixed pineal glands and cerebella were dehydrated and embedded in Histoplast paraffin (Biopack, Buenos Aires, Argentina). Five micrometer sections were incubated with one or a combination of the following primary antibodies: goat polyclonal anti-Iba1 1:200 (ab5076, Abcam, Cambridge, MA, USA); rabbit polyclonal anti-GABA 1:200 (AB5016, EMD Millipore, Bilerica, MA, USA); rabbit polyclonal anti-GABA<sub>A</sub>R $\alpha$ 1 1:200 (06-868, EMD Millipore); mouse monoclonal anti-GABA<sub>B</sub>1 1:200 (ab55051, Abcam); mouse monoclonal anti-glutamic acid decarboxylase 1 (GAD67) 1:200 (ab26116, K-87, Abcam); rabbit polyclonal anti-G $\alpha$  1:200 (07-634, EMD Millipore); rabbit polyclonal anti-Pax6 1:200 (Previously Covance PRB-278P, BioLegend, San Diego, CA, USA); mouse monoclonal anti-neuronal class III  $\beta$ -tubulin (Tuj1) 1:500 (Previously Covance MMS-435P, BioLegend); mouse polyclonal anti-tyrosine hydroxylase (TH) 1:200 (provided by Dr. A.M. Seltzer, IHEM, Mendoza, Argentina), and mouse monoclonal anti-vimentin (VIM) 1:200 (V6630, Sigma-Aldrich). Isolectin GS-IB4 (IB4) from *Griffonia simplicifolia* conjugated with Alexa Fluor 488 1:200 (I21411, Life Technologies-Invitrogen, Buenos Aires, Argentina) was also used. Nonspecific binding was defined by omitting the primary antibody. The secondary antisera included anti-rabbit conjugated with Alexa Fluor 488, anti-mouse labeled with the Cy3 fluorophore, Alexa Fluor 647-conjugated anti-goat, and biotinylated antibodies, Jackson ImmunoResearch Laboratories Inc. (West Grove, PA, USA) and Vector Laboratories Inc. (Burlingame, CA, USA), dilution 1:200. When required, fluorescein and Texas Red-conjugated streptavidins were used, Vector Laboratories Inc., dilution 1:200. Sections were mounted in the presence of the nuclear dye DAPI (D1306, Life Technologies-Invitrogen) and then analyzed using an Olympus FluoView FV-1000 confocal microscope (Olympus America Inc., Center Valley, PA, USA); images were processed with MacBiophotonic Image J and edited with Adobe Photoshop 7.0 (Adobe Systems Inc., San Jose, CA, USA). The percentage of GABAergic cells in the adult pineal gland was determined after immunolabeling pineal gland sections both for GABA and the biosynthetic enzyme GAD67 and counterstaining with DAPI. Although the number of these cells is low, they were identified not only by the simultaneous presence of both GABAergic markers but also by their characteristic nuclei and interstitial localization. Images acquired using a 60 $\times$  objective and a 2 $\times$  digital zoom were analyzed for this identification. Ten pineal glands were studied, five from each ZT. The number of GABAergic cells did not vary significantly between ZTs so all the data were combined.

## Western blot

Analysis of the enzyme GAD67 via Western blot was as described [32]. The procedure was modified for GABA receptor subunits to reduce non-specific binding and to facilitate their visualization. For GABA<sub>A</sub>R $\alpha$ 1 and GABA<sub>B</sub>1, whole protein extracts were made in 1× RIPA buffer (10×: 50 mM Tris-HCl, 150 mM NaCl, 1% NP40, 0.5% sodium deoxycholate, 0.1% SDS, pH 7.5) supplemented with phenylmethylsulfonyl fluoride (PMSF) and sodium orthovanadate. Protein concentrations were estimated using a Qubit 2.0 Fluorometer (Thermo Fisher Scientific Inc., Carlsbad, CA, USA). Proteins (10–30 µg per lane from cerebellum and 100–120 µg per lane from pineal gland pools) were separated by 7.5–12.5% SDS-polyacrylamide gel electrophoresis, transferred to PVDF membranes by electroblotting, and incubated with blocking solution [5% w/v of bovine serum albumin (BSA) in phosphate-buffered saline with 0.05% Tween-20]. Subsequently, membranes were incubated with the primary antibodies diluted in blocking solution: anti-GAD67 1:2000, anti-GABA<sub>A</sub>R $\alpha$ 1 1:1000, anti-GABA<sub>B</sub>1 1:1000 and rabbit polyclonal anti-actin 1:3000 (A 2066, Sigma-Aldrich). A lane with cerebellar whole proteins incubated under the same conditions as the samples with omission of the primary antibody was routinely included in every WB as negative control, and actin served as a loading control. The secondary antisera included anti-rabbit and anti-mouse antibodies conjugated with horseradish peroxidase (HRP) (Jackson ImmunoResearch Laboratories Inc.), dilution 1:10000. Protein bands were visualized with the LAS-4000 system (Fujifilm) after a chemiluminescent reaction (WBKLS0100, EMB Millipore).

## Electrophysiology and calcium measurement

All physiological experiments were performed on single isolated pinealocytes, the predominant cell type in the pineal gland [8]. When the pinealocytes were cultured on coverslips, they were readily identified by tiny spots on the membrane, which may reflect membrane blebs, folds, or microvilli on the cell surface [34]. They are round and stand up above the other adherent flat cells of the culture. Our trituration process produced mostly small clusters of pineal cells and a few single cells on each coverslip chip. We recorded from these single cells. Ionic currents under voltage clamp were measured in the whole-cell configuration using an EPC-9 patch-clamp amplifier (HEKA Electronic, Bellmore, New York, USA) with a low-pass filter frequency of 1 kHz and a sampling rate of 5 kHz [35]. When filled with the pipette solution, patch pipettes had a resistance of 4 – 6 MΩ. Series resistance and cell capacitance were compensated by at least 75%. Often here, we convert the current to current density by dividing by cell capacitance (pA/pF) to compensate for different pinealocyte membrane areas. The cell capacitance was typically on the order of 12–24 pF [36, 37]. The low-Cl<sup>-</sup> pipette solution for perforated patch, had a 10 mV junction potential against the bath solution that has been corrected where we report membrane potentials in the text from voltage-clamp or current-clamp experiments. Electrical and calcium recordings were performed at room temperature (22 – 24°C) soon after removal from the incubator. Perforated-patch recordings were obtained using identical methods with gramicidin (Sigma-Aldrich) dissolved in dimethylsulfoxide (Sigma-Aldrich) (50 mg/ml) then diluted in the pipette filling solution to a final concentration of 50 µg/ml. Gramicidin makes selective cation channels in the membrane patch not requiring mechanical rupture of the plasma membrane. The membrane access resistance was monitored to evaluate the

progress of perforation, which usually took more than 20 min. Pinealocytes exhibited very large outward potassium currents when depolarized [34, 36, 38] so to isolate the GABA-induced currents required subtracting records with and without GABA. To reduce these  $K^+$  currents, we used internal solutions containing  $Cs^+$  instead of  $K^+$  when possible.

To measure intracellular  $Ca^{2+}$  concentration  $[Ca^{2+}]_i$ , cells were loaded with 2  $\mu M$  fura-2-AM in saline solution for 45 min at room temperature. Cells were incubated in a dye-free solution for an additional 20 min to allow complete de-esterification of AM esters by endogenous esterases. Single pinealocytes were imaged by microscope (Nikon TE2000-U, Melville, NY, U.S.A.) equipped with a Polychrome monochromator (Polychrome IV; TILL Photonics, Graefelfing, Germany) and CCD camera (Photometrics, Tucson, AZ, USA). The excitation wavelengths were 340 and 380 nm, and fluorescence emission was collected at 510 nm every 1 s using Metafluor software (Molecular Devices, Sunnyvale, CA, USA). Background fluorescence from cell-free areas was used for correction. The ratio of fluorescence emitted by 340- and 380-nm excitations (F340/F380) was calculated off line using Excel (Microsoft, Redmond, USA) and plotted with Igor.

### Measurement of stimulated melatonin secretion

Pineal glands rapidly isolated at ZT2.5-4 were kept at 37°C in the 5%  $CO_2$  incubator in M199 medium for 48 or 72 h of conditioning, during which time glands were washed twice a day to remove any residual secretions. It is conventional to wait at least two days before studying NE-stimulated melatonin secretion *in vitro* in order to allow time for degeneration of the cut nerve endings within the pineal gland that release NE and other neuromodulators. In control experiments we have found that spontaneous melatonin release persists at least 24 h. After the conditioning period, glands were incubated in 96-well plate, one gland per well in 200  $\mu l$  medium. At the end of each 2 or 3 h sample period each gland was transferred briefly to a 90 mm dish with a small wire loop for quick agitation and washing several times before being moved to a new sampling well with the appropriate solution and returned to 37°C. The 200  $\mu l$  medium from the previous sample well was collected and frozen for later chromatographic analysis for 5-HT, NAS, melatonin (MEL), and GABA. Chromatographic separation was performed at ambient temperature using a C18 column (Waters Acquity UPLC Protein BEH C18, 300Å, 1.7  $\mu m$ , 2.1 mm  $\times$  100 mm, Waters Corporation, Milford, MA, USA). A Waters Acquity FTN autosampler set at 4°C injected 10  $\mu l$  of sample into the UPLC/MS. For chromatography the mobile phase consisted of 8 min runtime at a flow rate of 0.3 ml/min by a Waters Acquity UPLC. The gradient was initiated with 10 mM formic acid in water/10 mM formic acid in acetonitrile (98:2 v/v), held for 1 min, then increased to 2:98 v/v over 4 min and held for another minute before re-equilibration to starting conditions for 2 min. For quantitative analysis a Waters XEVO TQ-S MS/MS in Multiple Reaction Monitoring (MRM) using electrospray positive ion mode monitored the effluent. The MRM parameter settings are listed in Table S1. The internal standards included with the samples were deuterated d4-melatonin and d4-serotonin (C/D/N Isotopes Inc., Pointe-Claire, Quebec, Canada). To account for minor differences in pineal gland sizes (<30%) the DNA content of each pineal gland was measured and its mass-spectroscopy results were scaled by the DNA content in the largest gland. The mean recovered DNA content corresponded to about  $2.0 \pm 0.1 \times 10^6$  2N rat genomes per pineal gland (n = 18).

## Statistical analysis

Results are expressed as mean  $\pm$  standard error of mean (SEM); n is the number of independent cells or pineal glands. Student's t-test and ANOVA were used to test the difference between two and multiple sample groups, respectively.  $P < 0.05$  (\*) or  $P < 0.01$  (\*\*) were regarded as significant.

## Results

In order to describe signaling by GABA in the adult pineal gland, we hoped to identify its sources, receptors, and cellular effects. We started by demonstrating and characterizing GABAergic markers and cells. Western blot analysis of cytoplasmic homogenates from the pineal gland and cerebellum identified expression of the GABA biosynthetic enzyme GAD67 in both organs (Fig. 1A). A band around 67 kDa was observed in the pineal gland at both ZTs, with a slight relative increase at ZT6 compared to ZT18, whereas a characteristic three-band pattern was present in cerebellum [32]. GAD67 was also found by immunohistochemistry. As a positive control, Purkinje cells of the cerebellum, well known to be GABAergic, were highly positive for this enzyme (Fig. 1B). In the adult pineal gland, two sources of local GABA were identified by double immunolabeling for GABA itself and its generating enzyme GAD67: central GABAergic nerve fibers and a subpopulation of interstitial cells. The GAD67-immunoreactive nerve fibers were less abundant than the tyrosine hydroxylase-positive sympathetic ones, and were mainly perivascular (Fig. 1D–D'). The sparse GABAergic interstitial cells were also positive for the intermediate filament protein vimentin (Fig. 1E–I<sup>2</sup>). These GABAergic interstitial cells were not immunolabeled for Pax6, an essential determinant for initial establishment of pinealocyte specification that is still expressed in a subtype of perivascular cells in the adult pineal gland, or for Iba1, a marker of microglial cells (Fig. 1J–K). Thus the GABAergic cells are a separate interstitial cell type, most likely outside the pinealocyte lineage. Their nuclei are round or oval with a dense karyoplasm and their cytoplasm often exhibits a small number of thick projections in close proximity with blood vessels.

Now we turn to receptors. The presence of GABA receptors in the adult pineal gland was suggested by several studies, but to the best of our knowledge not previously demonstrated by immunolabeling or electrophysiology. We considered one ionotropic receptor subunit (GABA<sub>A</sub>R $\alpha$ 1) and one metabotropic receptor subunit (GABA<sub>B</sub>1). With an anti-GABA<sub>A</sub>R $\alpha$ 1 antibody, we confirmed immunoreactivity by Western blot and by immunohistochemistry (Fig. 2). A band around 51 kDa was clearly identified in cerebellum and in midday and midnight pineal glands (Fig. 2A). Again there were subtle but consistent differences between ZTs. Cerebellar sections immunolabeled for GABA<sub>A</sub>R $\alpha$ 1 exhibited a specific punctate pattern especially in the cytoplasm, surface, and dendritic tree of Purkinje cells (Fig. 2B). In pineal gland sections the most prominent GABA<sub>A</sub>R $\alpha$ 1 signal showed fine extensions often interlocked with and parallel to vimentin-positive blood vessels and in a more discontinuous way, to Tuj1-immunolabeled nerve fibers (Fig. 2D–E'). These nerve fibers were tyrosine hydroxylase-positive (sympathetic) or GAD67-immunoreactive (GABAergic) (Fig. 2F–G'). This receptor signal was not observed in the perinuclear cytoplasm of pinealocytes. Further electron or higher resolution optical microscope studies would be needed to ascertain



whether the GABA<sub>A</sub>R $\alpha$ 1 immunoreactivity is detectable in pinealocyte projections and membrane. The metabotropic GABA receptor subunit B1 was also studied (Fig. S1). A band of around 100 kDa (expected size 108 kDa) was seen in cerebellum and pineal gland, with higher expression at ZT6; two additional bands with lower molecular weights were consistently stained in whole extracts from pineal glands without apparent daily differences (Fig. S1A). In cerebellum, the dendritic tree surface and the cytoplasm of the GABAergic Purkinje cells were highly immunoreactive for GABA<sub>B</sub>1 (Fig. S1B). In the adult pineal gland, we found GABA<sub>B</sub>1 in a subpopulation of interstitial cells immunoreactive for Pax6 and in blood vessel walls, including at the membrane level (Fig. S1D–G). No specific GABA<sub>B</sub>1 signal was observed in the cytoplasm or the surface of pinealocytes.

Having discriminated the localization of molecules of GABAergic signaling in the pineal gland, we looked for actions of GABA and related compounds on isolated single pinealocytes. For electrophysiology, we were restricted to studying the round pinealocytes since other pineal cell types are much flatter and usually ramified and difficult to patch clamp on a coverslip of dispersed living cells. See Material and Methods (Electrophysiology and calcium measurement) for description. The experiments began by measuring ionic currents in cells under whole-cell voltage clamp. To magnify possible responses of GABA<sub>A</sub> receptor Cl<sup>-</sup> channels, the membrane potential was held at -100 mV, and Cl<sup>-</sup> was used as the major anion in the whole-cell pipette (internal) solution. Figure 3A shows large inward membrane currents evoked in a graded manner by perfusing increasing concentrations of GABA. The current densities were not significantly different whether measured 24, 48, or 72 h after dissociation (24 h:  $-14.9 \pm 3.4$  pA/pF, n = 8; 48 h:  $-10.8 \pm 3.8$  pA/pF, n = 7; 72 h:  $-11.8 \pm 4.9$  pA/pF, n = 8). The 50% effective concentration EC<sub>50</sub> for GABA was 26.5  $\mu$ M (Fig. 3B). These inward currents were inhibited in a graded fashion by the GABA<sub>A</sub> antagonist bicuculline (Fig. 3C) with a 50% inhibitory concentration IC<sub>50</sub> of 1.7  $\mu$ M bicuculline (Fig. 3D). The GABA<sub>A</sub> antagonist picrotoxin blocked the channels opened by GABA (Fig. 3E). Note that the picrotoxin block and unblock are slow and stimulus dependent. During the first 5-s coapplication of picrotoxin (10  $\mu$ M) and GABA, the current is initially large but fades to a low level, and during the first 5-s GABA application without picrotoxin, the current is initially small and rises in a slow ramp. Subsequent GABA applications progressively relieve the block. These are the classical signs of slow use-dependent block, and signify that access to and from the blocking site requires open channels. With this behavior, we did not attempt to define an IC<sub>50</sub> for picrotoxin. Continuing with pharmacology, we sought deeper confirmation that the GABA-evoked currents are from ionotropic GABA<sub>A</sub> receptors and not from metabotropic GABA<sub>B</sub> receptors. Like GABA, the selective GABA<sub>A</sub> agonist muscimol (10  $\mu$ M) also evoked bicuculline-sensitive inward currents (Fig. 4A). But unlike GABA and muscimol, the selective GABA<sub>B</sub> agonist baclofen (Fig. 4B) and the selective GABA<sub>B</sub> antagonist CGP 55845 (Fig. 4C) evoked no current by themselves, nor did they inhibit the current evoked by GABA<sub>A</sub> agonists. If anything, CGP 55845 potentiated the GABA-evoked current (Fig. 4D and E). Thus the currents evoked by application of GABA exhibit the typical pharmacological profile of GABA<sub>A</sub> receptor channels.

To confirm the identification of functional GABA<sub>A</sub> receptors in a different way, we asked whether the ion channels are selective for Cl<sup>-</sup> ions. With the nearly symmetrical Cl<sup>-</sup>

concentrations used already, the evoked ionic current is inward at all negative internal potentials, crosses zero near 0 mV, and is outward at all positive potentials (Fig. 5A). Thus the reversal potential for current is near 0 mV as is expected for a  $\text{Cl}^-$ -selective channel with symmetrical  $\text{Cl}^-$  solutions; the inward electric current seen at -100 mV would then represent outward movement of the  $\text{Cl}^-$  anion from the cytoplasmic solution. For most intact cells, the intracellular  $\text{Cl}^-$  concentration is much lower than the external concentration, so in that more native condition without whole-cell dialysis, the inward electric current would be expected to be smaller and the chloride equilibrium potential should lie negative from 0 mV. By using the perforated-patch configuration of the patch-clamp electrode, making electrical access pores in the membrane patch with gramicidin (a cation channel), we could record without disturbing the natural anion concentrations of the pinealocytes. In this configuration, the reversal potential for GABA-evoked currents was negative (-38 mV, Fig. 5B, red), and when the external  $\text{Cl}^-$  was also lowered, the reversal potential shifted back closer to 0 mV (Fig. 5B, purple). These properties are those expected for a  $\text{Cl}^-$ -selective ion channel, and they show that pinealocytes normally have a low intracellular  $\text{Cl}^-$  concentration.

Finally we turn to several, more functional questions. An ion channel with a reversal potential of -40 mV, should partially depolarize resting pinealocytes that have a -50 to -60 mV resting membrane potential and should partially repolarize pinealocytes that have been strongly depolarized by other treatments. We start with treatments with elevated  $\text{K}^+$ , which depolarize the membrane. Figure 6A shows that perfusion with a 30 mM  $\text{K}^+$  medium depolarizes pinealocytes to near -20 mV. GABA then repolarizes the membrane to near -40 mV despite elevated  $\text{K}^+$ , and bicuculline partly antagonizes this effect of GABA. These large depolarizations with KCl suffice to open voltage-gated  $\text{Ca}^{2+}$  channels in the membrane and evoke rises of intracellular  $\text{Ca}^{2+}$  (Fig. 6B; and Yoon et al. 2014 [36]). GABA counteracts the depolarization enough so that fewer  $\text{Ca}^{2+}$  channels are opened and the  $\text{Ca}^{2+}$  rise is smaller (Fig. 6C). This GABA effect is antagonized by bicuculline. Similarly the depolarizing neurotransmitter acetylcholine acting through nicotinic receptors depolarizes pinealocytes enough to open voltage-gated  $\text{Ca}^{2+}$  channels and evoke rises of intracellular  $\text{Ca}^{2+}$  (Fig. 6D; and Yoon et al. 2014 [36]). Again GABA reduces the  $\text{Ca}^{2+}$  signals. We could not test the effect of bicuculline in this experiment since it also blocks nicotinic ACh receptors [39], an effect we verified. Thus the  $\text{GABA}_A$  receptors of pinealocytes are potent enough to turn off signaling by voltage-gated  $\text{Ca}^{2+}$  channels. Does GABA also modulate *in vitro* stimulated melatonin secretion? We checked for this using mass spectrometry to assay secretion from intact pineal glands that had been cultured for 48 or 72 hours. We measured the 5-HT, N-acetylserotonin (NAS), and melatonin secreted into the medium in response to NE alone, to NE plus GABA, to GABA alone, and to NE plus acetylcholine (Fig. S2). The first experiment applied 2  $\mu\text{M}$  NE and 40  $\mu\text{M}$  GABA to pineal glands from 6-week old rats. As expected, NE alone stimulated strong secretion of NAS and melatonin after a 2-hour silent interval during which gene expression for the critical AANAT enzyme is induced (Fig. S2A). When NE was removed from the medium after the 5-hour NE treatment, the NAS and melatonin secretion continued to rise for several hours and only gradually tapered off. However, coapplication in the bath of GABA did not change the stimulation by NE or speed the recovery (Fig. S2B), and GABA did not stimulate secretion by itself (Fig. S2C). When the gland was actively making NAS and melatonin, the secretion of their precursor, 5-HT,

tended to droop, but the effect was small. During the periods of stimulation, the secretion of all three indoleamines was in a similar range of a few nanograms per hour per gland as in previous work [21, 40]. Supposing that the NE stimulus in this experiment might have been too strong to be countered by GABA, we next lowered the NE concentration to 0.5  $\mu\text{M}$  and raised the GABA concentration to 100  $\mu\text{M}$ . We also switched to 8-week old rats this time since we had begun to observe in the few electrophysiology experiments we did on younger rats that the GABA-evoked currents were less reliable. We did not do a careful time series, but the GABA response may undergo maturation in young adults. Despite these changes, the secretory response to NE and the absence of effect of GABA were the same in the second experiment as before (Fig. S2D and E). This experiment also included a test of whether 100  $\mu\text{M}$  ACh could antagonize the stimulation by NE (Fig. S2F). It did not. Thus despite their powerful effects on the membrane potential and  $\text{Ca}^{2+}$  signaling, neither GABA nor ACh application seemed to affect evoked indoleamine secretion from 48–72-h cultured intact pineal glands.

## Discussion

We have identified several components of GABAergic signaling in the pineal gland. We found protein bands of appropriate molecular weight in Western blots with an antibody against the GABA synthetic enzyme GAD67. These results are consistent with reports of mRNA for *Gad1* (GAD67) and *Gad2* (GAD65) in the pineal gland [3, 28]. Double immunostaining for GABA and GAD67 is present in a small set of central mostly perivascular nerve fibers as well as in a minor population of vimentin-positive interstitial cells that is distinct from microglia and from potential pinealocyte precursors. GABA-stained cell bodies were not seen by Sakai et al. [25], but improved antibodies and immunohistochemical procedures, and the higher-resolution of confocal microscopy may have allowed us to visualize them. Presumably the two types of double-labeled cells, which we call GABAergic, may participate at least partially both in the avid  $^3\text{H}$ -GABA uptake reported decades ago in pineal glands [16], and said then to be uptake into “gliocytes”, as well as in the  $^3\text{H}$ -GABA release induced by  $\text{K}^+$  and  $\alpha$ -adrenergic agonists [21]. Mata et al. [17] concluded that there were no GABAergic nerve fibers in the gland because GAD activity persisted after treatments that severed pinealopetal fibers and allowed them to degenerate. However, if GAD is present both in pinealopetal fibers and in interstitial cells as we find, the persistent GAD activity could be explained.

Further, and consistent with mRNA studies [3, 26], we see appropriate immunoreactive bands in Western blots for the GABA<sub>A</sub> receptor subunit GABA<sub>A</sub>R $\alpha$ 1. Using this antibody, there is GABA<sub>A</sub>R $\alpha$ 1 staining in pineal gland sections in fine extensions near blood vessels, which we now suggest could be pinealocyte processes [7, 8, 10, 11], and also in close proximity to both sympathetic and GABAergic nerve fibers. The receptors on sympathetic nerve terminals could account for the observation that application of GABA or muscimol (but also baclofen) modifies the uptake and release kinetics of  $^3\text{H}$ -NE into the pineal gland, an effect partially blocked by bicuculline [21, 22]. The dominant effect is inhibitory. The transport  $V_{\text{max}}$  is increased, but the  $K_{\text{m}}$  is also increased. Since the cell bodies of most superior cervical ganglion neurons are well-known to respond strongly to GABA by opening  $\text{Cl}^-$ -permeable, bicuculline- and picrotoxin sensitive GABA<sub>A</sub> channels with a reversal

potential near  $-42$  mV [41], it is not surprising that they also express GABA<sub>A</sub> channels where they terminate in the pineal gland. The most abundant GABA<sub>A</sub> subunits in the superior cervical ganglion are (in order)  $\gamma 2$ ,  $\beta 3$ ,  $\gamma 3$ , and  $\alpha 1$  [42]. However, we are confident that our electrical records are from pinealocytes rather than e.g. interstitial cells or nerve fibers since isolated living pinealocytes are easy to recognize and patch clamp because of their round shape and higher number than other cell types in the gland [8], and after 2 days of dispersed culture, all broken nerve terminals should have degenerated [43]. The electrophysiology gives unambiguous functional evidence for the presence of GABA<sub>A</sub> receptors on pinealocytes including the appropriate pharmacological actions of GABA, muscimol, and picrotoxin (with use dependence, [44, 45]) coupled to robust opening of Cl<sup>-</sup>-selective ion channels. Because there are 19 genes for GABA<sub>A</sub> receptor subunits (at least 5 present in the pineal transcriptome) and we tried to localize only one of them, the total GABA receptor density and localization in the pineal gland may be more extensive than our images suggest. Only future experiments with a comprehensive panel of antibodies could answer such questions. In the rat pineal gland, the GABAergic nerve fibers do not form synapses [25]. Perhaps the signaling is more like volume transmission in the brain, which means that the typical trans-synaptic signals for postsynaptic receptor clustering would be absent. Therefore it is possible that GABA receptors in pinealocytes are more diffuse and harder to detect with antibodies than when aggregated at conventional neural inhibitory synapses. In the pineal gland, mRNA for GABA<sub>A</sub>R $\rho 1$  subunits is unusually abundant [3, 26, 27], as it is in retinal photoreceptors (to which pinealocytes are evolutionarily related, Klein [9]), but such inhibitory receptors (often called rho or GABA<sub>C</sub>) are not bicuculline sensitive [46]. Therefore somewhat surprisingly we probably were not detecting currents from rho subunits in our recordings. Instead we may have recorded from GABA<sub>A</sub> channels combining, among others, the  $\alpha 1$ -,  $\beta 3$ -,  $\gamma 2$ -, and/or  $\epsilon$  subunits seen in pineal gland transcriptome analyses [3, 26, 27]. Functional studies with diagnostic subunit-specific reagents would be needed for deeper analysis.

We also see appropriate immunoreactive bands in Western blots for GABA<sub>B1</sub> receptor subunits as well as immunostaining in interstitial cells. This is consistent with a report of mRNA for the GABA<sub>B1</sub> receptor subunit and its obligate partner GABA<sub>B2</sub> (*Gabbr1* and *Gabbr2*, respectively) in pineal extracts [3]. Our Western blots showed several bands in the pineal gland. The two higher molecular weight bands may represent tissue- and developmental stage-dependent splice variants as reported in brain before [47, 48]. Neurons of the superior cervical ganglion also express GABA<sub>B</sub> receptors [49] and might retain them at their nerve terminals in the pineal gland. Typically in neurons, GABA<sub>B</sub> receptors can mediate presynaptic inhibition of transmitter release, so like the presynaptic ionotropic GABA<sub>A</sub> receptors, the metabotropic GABA<sub>B</sub> receptors can modulate sympathetic release of NE and thus reduce melatonin output in the gland [21]. We would not have seen such effects in our melatonin secretion experiments both because we applied NE exogenously and because the nerve terminals would be gone in the 48–72-h cultured glands. So far, we have not detected electrophysiological evidence for functional GABA<sub>B</sub> receptors on pinealocytes, consistent with a lack of immunoreactivity for this metabotropic subunit in their cytoplasm and membrane.

The previous searches for effects of GABA on melatonin secretion are contradictory and report all possibilities as described in the Introduction: (i) enhancement [20], (ii) no effect [17], and (iii) inhibition [20–22] of AANAT activity or melatonin synthesis and secretion, all with subtle differences in protocols. They may all be correct depending on conditions. Our protocol, which is most like that of Mata et al. [17] using glands cultured for several days, did not show any GABA action on stimulated melatonin secretion in two trials as they also found. Freshly isolated glands used exclusively by Balemans et al. [20] and Rosenstein [21, 22] would include functional nerve fibers with their NE and GABA uptake and release mechanisms that may also be modulated by GABA, whereas in long-cultured glands, nerve fibers will be gone but functional pinealocytes remain. In these earlier experiments, because of continued secretion of NE in fresh glands, the background melatonin secretion was much higher than in ours and the dynamic increase of stimulated secretion was only 2–3 fold instead of 100-fold. Future experiments will be needed to verify that several-hour experiments on intact glands (ours and those of Mata et al., Balemans et al. and Rosenstein [17, 20–22]) are not significantly limited by a combination of the following factors: possible insufficient access of GABA to the pinealocytes, or avid local clearance by uptake into cells, or acute desensitization of the receptors. If GABA is normally delivered by nerve fibers, it may be released in a pulsatile pattern rather than as a desensitizing constant application. What is GABA doing for pineal gland physiology? There probably are multiple roles since, as we show, several cell types in the intact gland contain GABA, can synthesize GABA, or have receptors for GABA. We will want to know what natural stimuli initiate release and clearance of GABA. Our functional assays for membrane potential changes and for intracellular calcium signals showed strong GABA effects so we anticipate that important roles will emerge. Perhaps the focus on melatonin release obscures other interesting actions. Rather than simple prevention of secretion, GABA may mediate more subtle fine tuning of NE release, adjusting timing and responsiveness of pinealocytes, or rather it may modulate the circadian activity of thyroid hormones by affecting the rhythmic expression of type II iodothyronine deiodinase [12, 13], or it might modulate the secretion of peptides within the gland [50], or it might underlie even longer term remodeling of the gland with time of day and season.

## Supplementary Material

Refer to Web version on PubMed Central for supplementary material.

## Acknowledgments

We thank Drs. William J. Spain, Christopher B. Ransom and Alicia M. Seltzer for reagents, Christopher Kushmerick for comments on the manuscript, Morten Møller, David C. Klein, and Andrea Meredith for expert advice, and Lea Miller for technical assistance. Supported by grants from the National Institute of General Medical Sciences of the NIH (R01GM-083913), PIP-CONICET 112-201101-00247 (<http://www.conicet.gov.ar>), PICT 2007-682 and 2012-174 ANPCyT (<http://www.agencia.mincyt.gov.ar>), and the Wayne E. Crill Endowed Professorship.

## References

1. MØLLER M. Fine structure of the pinealopetal innervation of the mammalian pineal gland. *Microsc Res Tech.* 1992; 21:188–204. [PubMed: 1606315]

2. SIMONNEAUX V, RIBELAYGA C. Generation of the melatonin endocrine message in mammals: a review of the complex regulation of melatonin synthesis by norepinephrine, peptides, and other pineal transmitters. *Pharmacol Rev.* 2003; 55:325–395. [PubMed: 12773631]
3. HARTLEY SW, COON SL, SAVASTANO LE, et al. Neurotranscriptomics: The Effects of Neonatal Stimulus Deprivation on the Rat Pineal Transcriptome. *PLoS One.* 2015; 10:e0137548. [PubMed: 26367423]
4. KLEIN DC. Arylalkylamine N-acetyltransferase: “the Timezyme”. *J Biol Chem.* 2007; 282:4233–4237. [PubMed: 17164235]
5. KLEIN DC, COON SL, ROSEBOOM PH, et al. The melatonin rhythm-generating enzyme: molecular regulation of serotonin N-acetyltransferase in the pineal gland. *Recent Prog Horm Res.* 1997; 52:307–357. discussion 357–358. [PubMed: 9238858]
6. YU H, DICKSON EJ, JUNG SR, et al. High membrane permeability for melatonin. *J Gen Physiol.* 2016; 147:63–76. [PubMed: 26712850]
7. ARSTILA AU. Electron microscopic studies on the structure and histochemistry of the pineal gland of the rat. *Neuroendocrinology.* 1967; 2(Suppl):1–101.
8. MØLLER M, BAERES FM. The anatomy and innervation of the mammalian pineal gland. *Cell Tissue Res.* 2002; 309:139–150. [PubMed: 12111544]
9. KLEIN DC. The 2004 Aschoff/Pittendrigh lecture: Theory of the origin of the pineal gland—a tale of conflict and resolution. *J Biol Rhythms.* 2004; 19:264–279. [PubMed: 15245646]
10. MCNULTY JA, FOX LM, SILBERMAN S. Immunocytochemical demonstration of nerve growth factor (NGF) receptor in the pineal gland: effect of NGF on pinealocyte neurite formation. *Brain Res.* 1993; 610:108–114. [PubMed: 8518918]
11. MCNULTY JA, TSAI SY, FOX LM, et al. Neurotrophic effects of the pineal gland: role of non-neuronal cells in co-cultures of the pineal gland and superior cervical ganglia. *J Pineal Res.* 1995; 19:40–50. [PubMed: 8609594]
12. GUERRERO JM, REITER RJ. Iodothyronine 5′-deiodinating activity in the pineal gland. *Int J Biochem.* 1992; 24:1513–1523. [PubMed: 1397480]
13. CHIK CL, PRICE DM, HO AK. Histone modifications on the adrenergic induction of type II deiodinase in rat pinealocytes. *Mol Cell Endocrinol.* 2011; 343:63–70. [PubMed: 21704117]
14. MORTENSEN M, PATEL B, SMART TG. GABA Potency at GABA<sub>A</sub> Receptors Found in Synaptic and Extrasynaptic Zones. *Front Cell Neurosci.* 2012; 6:1. [PubMed: 22319471]
15. HEANEY CF, KINNEY JW. Role of GABA<sub>B</sub> Receptors in Learning and Memory and Neuropsychological Disorders. *Neurosci Biobehav Rev.* 2016; 63:1–28. [PubMed: 26814961]
16. SCHON F, BEART PM, CHAPMAN D, et al. On GABA metabolism in the gliocyte cells of the rat pineal gland. *Brain Res.* 1975; 85:479–490. [PubMed: 234281]
17. MATA MM, SCHRIER BK, KLEIN DC, et al. On GABA function and physiology in the pineal gland. *Brain Res.* 1976; 118:383–394. [PubMed: 1009426]
18. EBADI M, CHAN A. Characteristics of GABA binding sites in bovine pineal gland. *Brain Research Bulletin.* 1980; 5:179–187. [PubMed: 7378857]
19. WANIEWSKI RA, SURIA A. Modulation of Cyclic GMP in the Rat Pineal Gland by GABA. *Brain Res Bull.* 1980; 5:1980.
20. BALEMANS MG, MANS D, SMITH I, et al. The influence of GABA on the synthesis of N-acetylserotonin, melatonin, O-acetyl-5-hydroxytryptophol and O-acetyl-5-methoxytryptophol in the pineal gland of the male Wistar rat. *Reprod Nutr Dev.* 1983; 23:151–160. [PubMed: 6844712]
21. ROSENSTEIN RE, CHULUYAN HE, PEREYRA EN, et al. Release and effect of gamma-aminobutyric acid (GABA) on rat pineal melatonin production in vitro. *Cell Mol Neurobiol.* 1989; 9:207–219. [PubMed: 2472890]
22. ROSENSTEIN RE, CHULUYAN HE, DIAZ MC, et al. GABA as a presumptive paracrine signal in the pineal gland. Evidence on an intrapineal GABAergic system. *Brain Res Bull.* 1990; 25:339–344. [PubMed: 2171722]
23. REDECKER P. Immunoreactivity for multiple GABA transporters (GAT-1, GAT-2, GAT-3) in the gerbil pineal gland. *Neurosci Lett.* 1999; 266:117–120. [PubMed: 10353341]

24. ECHIGO N, MORIYAMA Y. Vesicular inhibitory amino acid transporter is expressed in gamma-aminobutyric acid (GABA)-containing astrocytes in rat pineal glands. *Neurosci Lett.* 2004; 367:79–84. [PubMed: 15308302]
25. SAKAI Y, HIRA Y, MATSUSHIMA S. Central GABAergic innervation of the mammalian pineal gland: a light and electron microscopic immunocytochemical investigation in rodent and nonrodent species. *J Comp Neurol.* 2001; 430:72–84. [PubMed: 11135246]
26. BAILEY MJ, COON SL, CARTER DA, et al. Night/day changes in pineal expression of >600 genes: central role of adrenergic/cAMP signaling. *J Biol Chem.* 2009; 284:7606–7622. [PubMed: 19103603]
27. OCHOCINSKA MJ, MUÑOZ EM, VELERI S, et al. NeuroD1 is required for survival of photoreceptors but not pinealocytes: results from targeted gene deletion studies. *J Neurochem.* 2012; 123:44–59. [PubMed: 22784109]
28. MUÑOZ EM, BAILEY MJ, RATH MF, et al. NeuroD1: developmental expression and regulated genes in the rodent pineal gland. *J Neurochem.* 2007; 102:887–899. [PubMed: 17630985]
29. YAMADA H, YAMAMOTO A, TAKAHASHI M, et al. The L-type Ca<sup>2+</sup> channel is involved in microvesicle-mediated glutamate exocytosis from rat pinealocytes. *J Pineal Res.* 1996; 21:165–174. [PubMed: 8981261]
30. KIM MH, UEHARA S, MUROYAMA A, et al. Glutamate transporter-mediated glutamate secretion in the mammalian pineal gland. *J Neurosci.* 2008; 28:10852–10863. [PubMed: 18945893]
31. KOH DS, HILLE B. Modulation by neurotransmitters of catecholamine secretion from sympathetic ganglion neurons detected by amperometry. *Proc Natl Acad Sci U S A.* 1997; 94:1506–1511. [PubMed: 9037083]
32. BENITEZ SG, CASTRO AE, PATTERSON SI, et al. Hypoxic preconditioning differentially affects GABAergic and glutamatergic neuronal cells in the injured cerebellum of the neonatal rat. *PLoS One.* 2014; 9:e102056. [PubMed: 25032984]
33. CASTRO AE, BENITEZ SG, FARIAS ALTAMIRANO LE, et al. Expression and cellular localization of the transcription factor NeuroD1 in the developing and adult rat pineal gland. *J Pineal Res.* 2015; 58:439–451. [PubMed: 25752781]
34. AGUAYO LG, WEIGHT FF. Characterization of membrane currents in dissociated adult rat pineal cells. *J Physiol.* 1988; 405:397–419. [PubMed: 2855641]
35. HAMILL OP, MARTY A, NEHER E, et al. Improved patch-clamp techniques for high-resolution current recording from cells and cell-free membrane patches. *Pflugers Arch.* 1981; 391:85–100. [PubMed: 6270629]
36. YOON JY, JUNG SR, HILLE B, et al. Modulation of nicotinic receptor channels by adrenergic stimulation in rat pinealocytes. *Am J Physiol Cell Physiol.* 2014; 306:C726–735. [PubMed: 24553185]
37. YU H, SEO JB, JUNG SR, et al. Noradrenaline upregulates T-type calcium channels in rat pinealocytes. *J Physiol.* 2015; 593:887–904. [PubMed: 25504572]
38. CASTELLANO A, LOPEZ-BARNEO J, ARMSTRONG CM. Potassium currents in dissociated cells of the rat pineal gland. *Pflugers Arch.* 1989; 413:644–650. [PubMed: 2726427]
39. DEMURO A, PALMA E, EUSEBI F, et al. Inhibition of nicotinic acetylcholine receptors by bicuculline. *Neuropharmacology.* 2001; 41:854–861. [PubMed: 11684149]
40. CHATTORAJ A, LIU T, ZHANG LS, et al. Melatonin formation in mammals: in vivo perspectives. *Rev Endocr Metab Disord.* 2009; 10:237–243. [PubMed: 20024626]
41. ADAMS PR, BROWN DA. Actions of gamma-aminobutyric acid on sympathetic ganglion cells. *J Physiol.* 1975; 250:85–120. [PubMed: 1177140]
42. LIU ZF, BURT DR. GABAA receptor subunit mRNAs in rat superior cervical ganglia. *Pharmacology.* 1999; 58:51–58. [PubMed: 9831831]
43. SAVASTANO LE, CASTRO AE, FITT MR, et al. A standardized surgical technique for rat superior cervical ganglionectomy. *J Neurosci Methods.* 2010; 192:22–33. [PubMed: 20637235]
44. NEWLAND CF, CULL-CANDY SG. On the mechanism of action of picrotoxin on GABA receptor channels in dissociated sympathetic neurones of the rat. *J Physiol.* 1992; 447:191–213. [PubMed: 1317428]

45. YOON KW, COVEY DF, ROTHMAN SM. Multiple mechanisms of picrotoxin block of GABA-induced currents in rat hippocampal neurons. *J Physiol.* 1993; 464:423–439. [PubMed: 8229811]
46. FEIGENSPAN A, WASSLE H, BORMANN J. Pharmacology of GABA receptor Cl<sup>-</sup> channels in rat retinal bipolar cells. *Nature.* 1993; 361:159–162. [PubMed: 7678450]
47. ISOMOTO S, KAIBARA M, SAKURAI-YAMASHITA Y, et al. Cloning and tissue distribution of novel splice variants of the rat GABAB receptor. *Biochem Biophys Res Commun.* 1998; 253:10–15. [PubMed: 9875211]
48. FRITSCHY JM, MESKENAITE V, WEINMANN O, et al. GABAB-receptor splice variants GB1a and GB1b in rat brain: developmental regulation, cellular distribution and extrasynaptic localization. *Eur J Neurosci.* 1999; 11:761–768. [PubMed: 10103070]
49. FILIPPOV AK, COUVE A, PANGALOS MN, et al. Heteromeric assembly of GABA<sub>B</sub>R1 and GABA<sub>B</sub>R2 receptor subunits inhibits Ca<sup>2+</sup> current in sympathetic neurons. *J Neurosci.* 2000; 20:2867–2874. [PubMed: 10751439]
50. KARLSEN AS, RATH MF, ROHDE K, et al. Developmental and diurnal expression of the synaptosomal-associated protein 25 (Snap25) in the rat pineal gland. *Neurochem Res.* 2013; 38:1219–1228. [PubMed: 23135794]



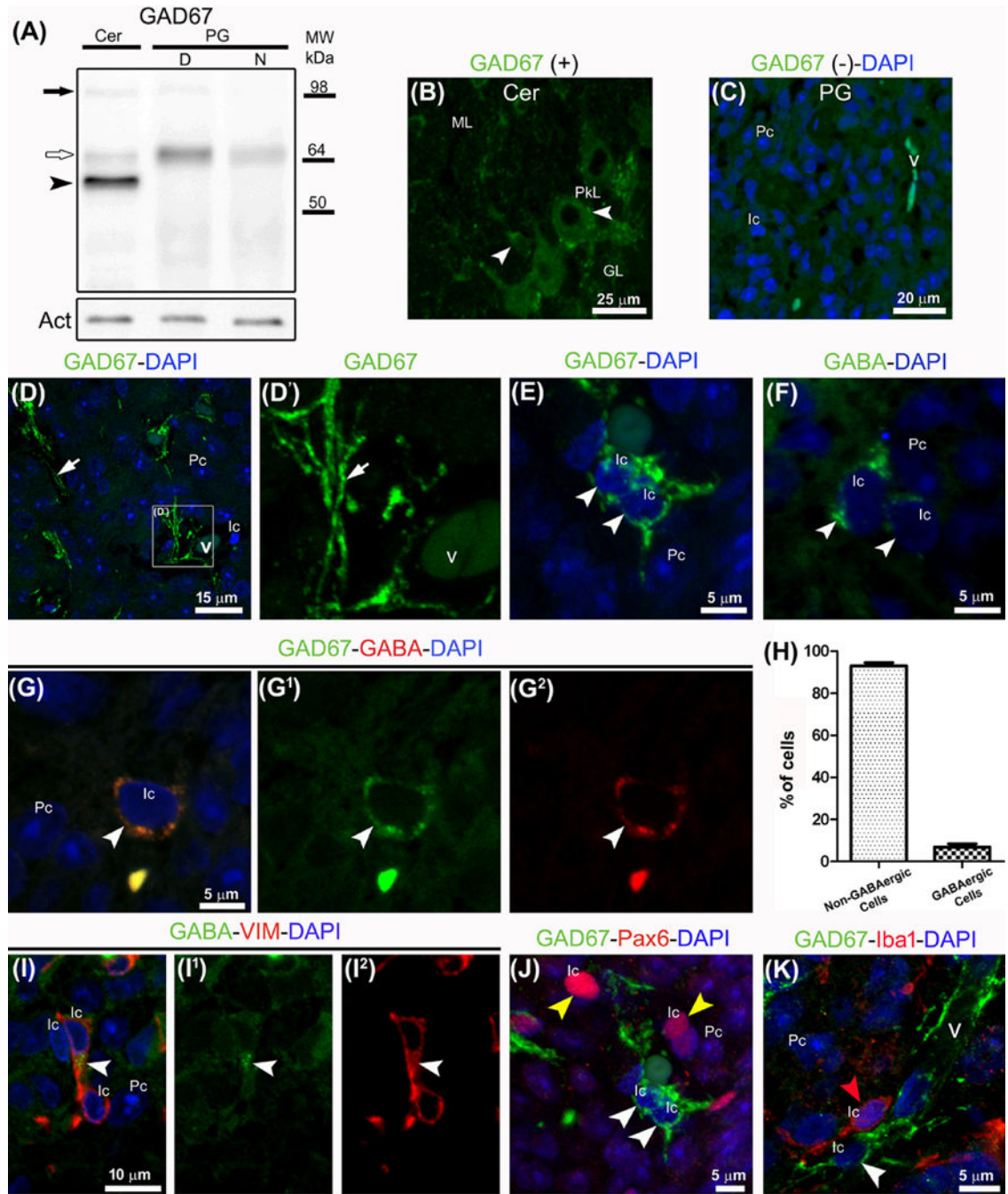


**Fig. 1.** GABA is synthesized in the adult rat pineal gland as revealed by immunoreactive GAD67 in Western blot and immunohistochemistry. (A) Representative blot of cytoplasmic extracts from cerebellum (Cer) and pineal gland (PG) pools collected at midday (D) and midnight (N). A 67 kDa band (white arrow) is prominent in pineal gland; cerebellum shows additional bands around 55 kDa (black arrowhead) and 110 kDa (black arrow). Actin (Act) served as a loading control. (B–K) Cerebellar and pineal gland sections immunolabeled for GAD67 (green), GABA (green or red), vimentin (VIM, red), Pax6 (red) and Iba1 (red); DAPI (blue)

was used as general nuclear dye. (B, C) Cerebellar and pineal gland sections incubated with and without anti-GAD67 antibody, respectively. (B) GAD67-positive cells in the Purkinje cell layer (PkL) and molecular layer (ML) are indicated by white arrowheads. (C) Pinealocytes (Pc) and interstitial cells (Ic) are distinguished by their differential nuclear morphology and karyoplasm density. (D–G<sup>2</sup>, I–K) GABAergic nerve fibers (white arrows) in close proximity to blood vessels (v) and interstitial GABAergic cells (white arrowheads) positive for GAD67, GABA, and VIM. These cells are distinct from interstitial cells immunoreactive for Pax6 (yellow arrowheads) or Iba1 (red arrowhead). (H) The GABAergic cells represent ~5% of the total cells in the pineal gland. Abbreviations: GL, cerebellar granular layer; MW, molecular weight. (B) 4× digital zoom of a 40× image. (C) 1.1× magnification of a 60× image. (D) 2× digital zoom of a 100× image. (D′) 2× enlargement of the inset shown in D. (E–G<sup>2</sup>) 4× digital zooms from 60× images. (I–I<sup>2</sup>, J, K) 3×, 3.4× and 3.8× enlargements from 60× images.

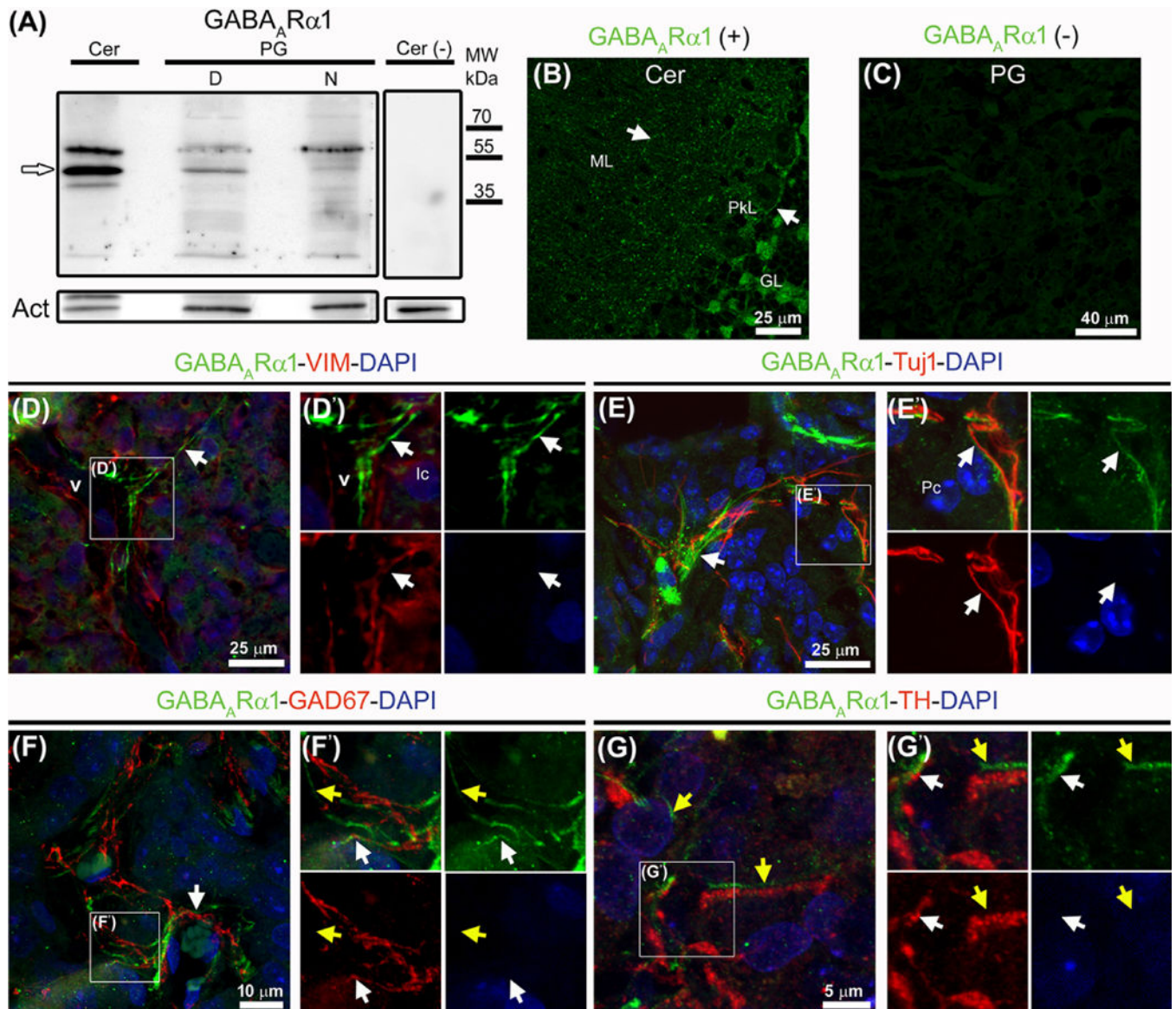


**Fig. 2.** Western blot and immunohistochemistry reveal the ionotropic receptor subunit  $\text{GABA}_A\text{R}\alpha 1$  in the adult rat pineal gland. (A) A band around 51 kDa (white arrow) seen in whole extracts from cerebellum (Cer) and pineal gland (PG) pools at midday (D) and midnight (N). Omission of the primary antibody and actin (Act) served as negative and loading controls, respectively. (B–G') Immunolabeling for  $\text{GABA}_A\text{R}\alpha 1$  (green), vimentin (VIM, red), Tuj1 (red), GAD67 (red), and tyrosine hydroxylase (TH) (red); nuclei were counterstained with DAPI (blue). (B) Punctate pattern of the ionotropic subunit in the cytoplasm, surface and dendritic tree of Purkinje cells (PkL, white arrows). (C) Pineal gland without primary antibody. (D–G') In pineal gland sections a specific signal for  $\text{GABA}_A\text{R}\alpha 1$  is seen as extensions often interlocked with or parallel to VIM-positive blood vessels (v) and in a more discontinuous way, to sympathetic and GABAergic nerve fibers (white arrows). A signal not associated directly with pineal gland innervation is marked with yellow arrows. (D', E', F',

G') Higher magnifications of the insets shown in D–G. Abbreviations: GL, cerebellar granular layer; Ic, interstitial cells; ML, cerebellar molecular layer; MW, molecular weight; Pc, pinealocytes. (B) 1.1× magnification of a 60× image. (D, E) 2× digital zooms of 60× images. (D', E') 2× enlargements of the insets shown in D and E. (F) 1.2× magnification of a 60× image. (G) 4× digital zoom of a 100× image. (F', G') 2× and 1.5× enlargements of the insets shown in F and G, respectively.

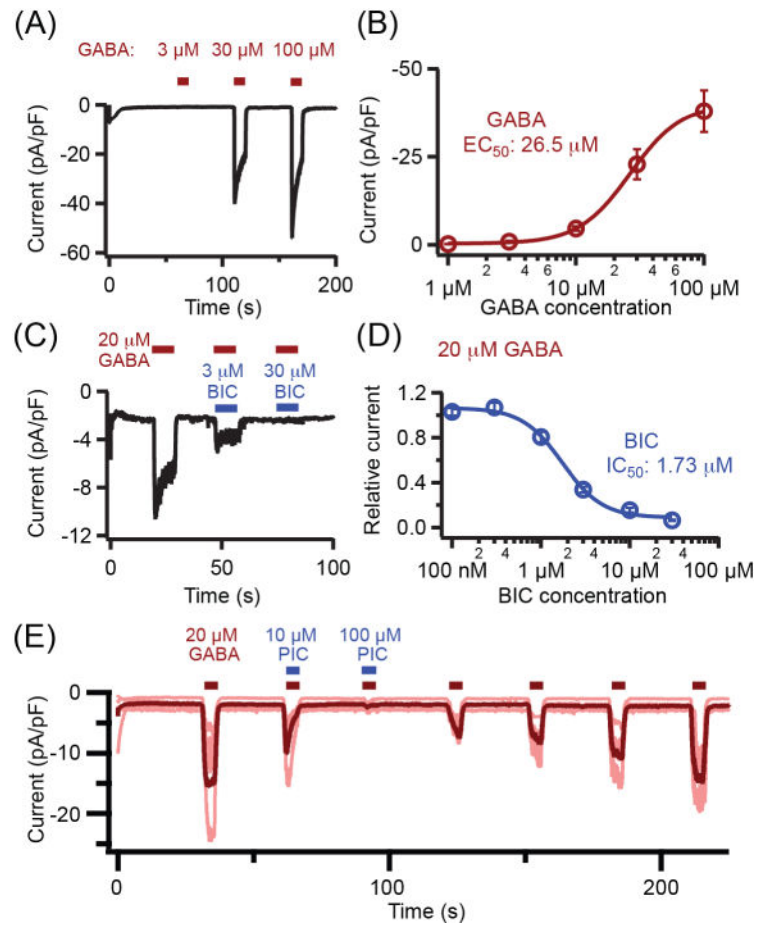


**Fig. 3.** GABA evokes inward ionic currents blocked by GABA<sub>A</sub> antagonists in pinealocytes under whole-cell patch-clamp recording. (A) Representative trace of membrane currents evoked as increasing concentrations of GABA are perfused in the bath. (B) GABA concentration-response relation for peak evoked current. ( $n = 4-5$  pinealocytes). (C) Sample trace of three coapplications of 20 μM GABA with 0, 3, or 30 μM bicuculline (BIC). (D) The inhibitory BIC concentration-response relation during coapplication with 20 μM GABA. ( $n = 4-5$  pinealocytes). (E) Picrotoxin (PIC) blocks GABA-evoked currents. ( $n = 5$  pinealocytes). Conditions for all panels: holding potential  $-100$  mV; approximately equal chloride concentrations inside and outside. Bars show mean  $\pm$  SEM. Age of rats: A, B, C, D, 7 weeks; E, 10 weeks.

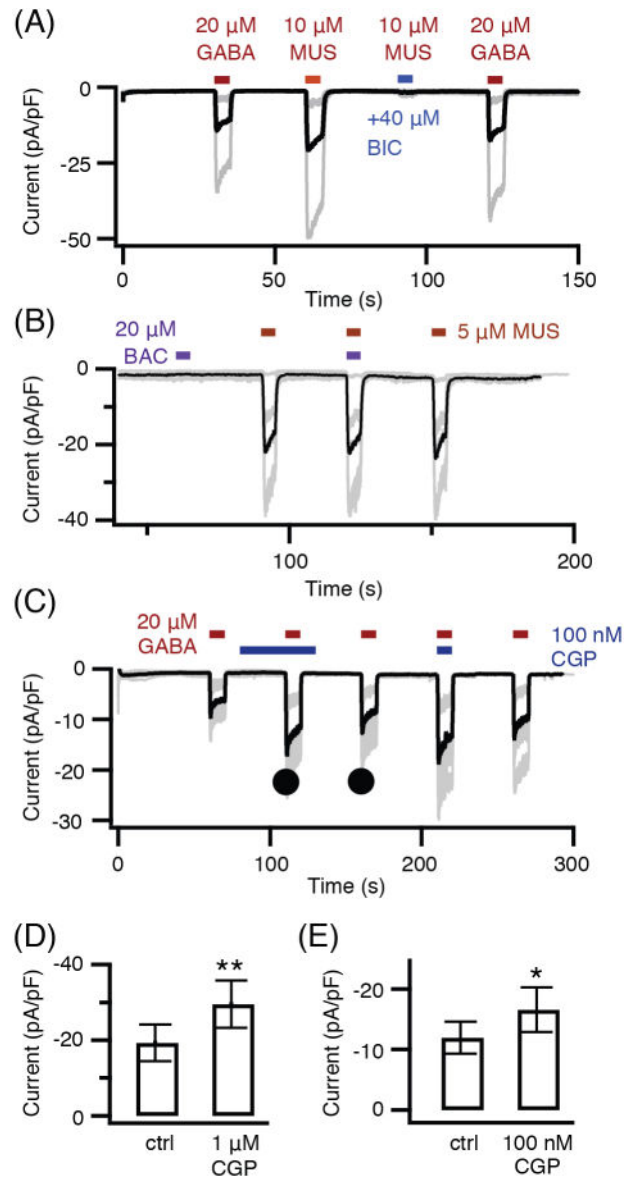


**Fig. 4.** GABA<sub>A</sub> agonists evoke current and a GABA<sub>B</sub> agonist does not. (A) Muscimol (MUS) evokes bicuculline (BIC)-sensitive inward currents. Individual recordings are shown as gray lines and the averaged record as a black line. ( $n = 3$  pinealocytes) (B) Baclofen (BAC) evokes no current and does not antagonize muscimol-induced current. ( $n = 5$  pinealocytes) (C) GABA<sub>B</sub> antagonist CGP 55845 (CGP) evokes no current and does not antagonize GABA-induced current. ( $n = 5$  pinealocytes) (D) and (E) comparison of mean GABA current densities without and with two concentrations of CGP 55845 measured as marked by filled circles in C. Bars show mean  $\pm$  SEM. \*  $P < 0.05$ , \*\*  $P < 0.01$ . Conditions for all panels: whole-cell recording; holding potential  $-100$  mV; approximately equal chloride concentrations inside and outside. Age of rats: A, B, 10 weeks; C, D, E, 8 weeks.

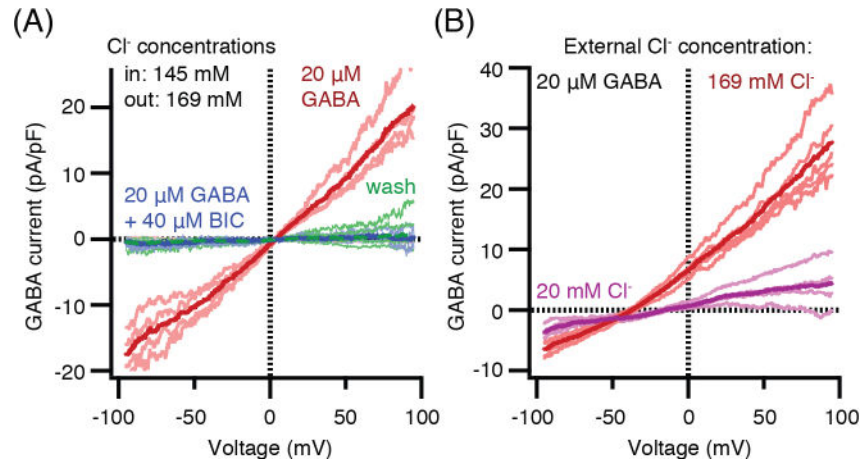


**Fig. 5.** Current-voltage relations of GABA-induced current with different  $\text{Cl}^-$  concentration gradients across the membrane. (A) Whole-cell recording and nearly symmetrical high- $\text{Cl}^-$  concentrations (red), block by 40  $\mu\text{M}$  bicuculline (BIC, blue), and final wash (green). ( $n = 4$  pinealocytes). (B) Gramicidin perforated-patch recording to preserve intracellular  $\text{Cl}^-$  levels. External solution is 169 mM  $\text{Cl}^-$  (red, reversal potential  $V_{\text{rev}} = -37.8 \pm 1.0$  mV) and changed to 20 mM  $\text{Cl}^-$  (purple,  $V_{\text{rev}} = -12.4 \pm 2.0$  mV). Chloride substitutes used are glutamate in pipette and gluconate in bath. ( $n = 5$  pinealocytes). All currents shown are difference currents, with-GABA minus without-GABA or for the “wash” curve, final record minus initial baseline. Individual recordings are shown as pale lines and averaged records as heavy lines. Age of rats: A, 9 weeks; B, 10 weeks.

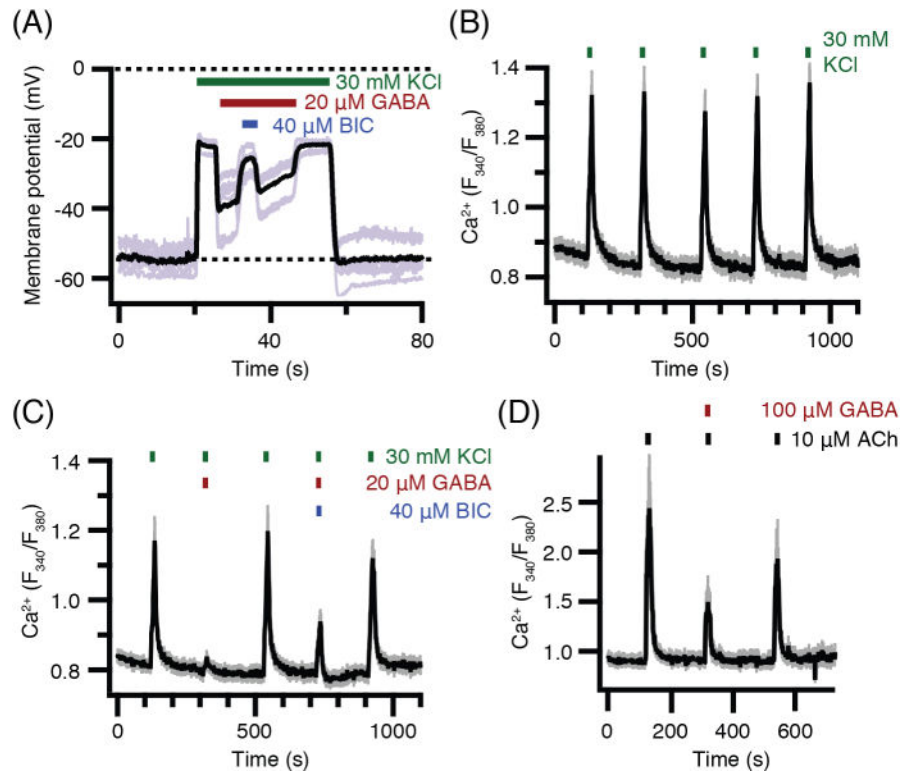


**Fig. 6.**

GABA suppresses KCl- and acetylcholine (ACh)-induced depolarization and calcium elevations. (A) Membrane potential recordings using perforated patch. KCl depolarizes the membrane, GABA partially repolarizes, and bicuculline (BIC) blocks the GABA effect. Five individual traces (gray) and their average (black). ( $n = 5$  pinealocytes). (B, C, D) KCl- and ACh-induced calcium elevations in intact fura-2-loaded pinealocytes. (B) Five control applications of 30 mM KCl. ( $n = 22$  pinealocytes). (C) Five applications of KCl variously mixed with GABA and bicuculline as marked showing strong suppression of Ca<sup>2+</sup> response by 20 μM GABA and partial antagonism by 40 μM bicuculline. (D) Three applications of acetylcholine (ACh) showing suppression of Ca<sup>2+</sup> response by 100 μM GABA. ( $n = 25$  pinealocytes). In (B) (C), and (D), traces include mean (black) and SEM (gray) at each time point. Age of rats: A, 10 weeks; B, C, 6 weeks; D, 8 weeks.